Journal of Thermal Analysis, Vol. 37 (1991) 1053-1064

CORRELATION BETWEEN PORE STRUCTURE AND LOW-TEMPERATURE DILATATION OF HYDRATED CEMENT PASTES AND MORTARS
Effect of cement type

Zs. E. Wagner

CENTRAL RESEARCH AND DESIGN INSTITUTE FOR SILICATE INDUSTRY BUDAPEST, H-1300, PF. 112, HUNGARY

(Received December 29, 1990)

The pore structure and low-temperature dilataion behaviour of a traditional hydrated Portland cement paste and a special cement paste of high initial strength were investigated.

The aim of the investigation was to demonstrate the role of the cement type in developing the pore structure and frost dilatation during the hydration process. The lower porosity and the higher strength of the special hydrated cement paste resulted in smaller frost dilatation effects in comparison with those of the traditional cement paste in the early stage of hydration.

Ensurance of the safety and durability of constructions is one of the typical problems in structural engineering. In this respect, the continued long-term integrity of the structure under service conditions is of vital importance for concretes and cement-containing materials. Frost action is one of the most important effects which must be taken into consideration when the service conditions of porous building materials exposed to weather changes are investigated.

The frost resistance of porous materials is influenced by several properties, e.g. strength, porosity, dilatation, etc. The experimental testing of constructions in service, together with investigations on laboratory models, can provide satisfactory answers in this field. The behaviour of concerete is influenced by the properties of the hydrated cement paste or mortar component of the material, and research on hydrated cement paste and mortar models could therefore contribute to the knowledge on concretes.

John Wiley & Sons, Limited, Chichester
Akadémiai Kiadó, Budapest

The aim of our work was to compare some properties of hydrated cement pastes and mortars at different stages of hydration, in order to acquire information about the correlation of these properties and frost resistance.

The pore size distribution and the low-temperature dilatation under saturated conditions were the two properties compared, as porosity is one of the major factors controlling the mechanical properties and resistance to frost action of cement pastes or mortars, while low-temperature dilatometry is an appropriate method of recording the change in size during frost attack.

The pore structure of hydrated cement pastes and mortars is influenced by the properties of the cement used, the water-to-cement ratio, the properties of the aggregate and the conditions of hydration. In order to obtain models with different pore structures, samples were made from two types of cement and by applying several *w/c* ratios. Different compacting conditions and different cement-to-aggregate ratios were also applied for the same reason.

In the present paper the influences of the cement type on the pore structure and the low-temperature dilatation behaviour of hydrated cement pastes in the early stage of hydration will be discussed.

Pore size ranges and water structures in hydrated cement pastes and mortars

It is known that the pore size distribution of hydrated cement pastes and mortars can be characterized by several pore size ranges. As the pore structure of materials containing hydrated cement paste could not be described by applying Dubinin's classification of pore sizes, Parcevaux recently proposed a model to describe the pore size distribution with the characteristics as follows [1, 2]:

- surface porosity in the range larger than 1 μm, this not being interconnected to the matrix of the sample through pores of the same size;

- macroporosity, in the pore diameter range 100–1000 nm, i.e. the wide pores between cement grains;

- mesoporosity, in the pore diameter range 10–100 nm, i.e. the porosity between more or less hydrated cement grains;

- microporosity, in the pore diameter range 1–10 nm, i.e. the internal porosity of hydration products.

The structure of water saturating a hydrated cement paste is influenced by the pore size distribution on the paste. On the basis of the results of thermoanalytical investigations, Dorner and Setzer distinguished four types of water structure relating to the four characteristic pore size ranges [3]. The difference in structure is detectable via the lowering of the temperature of ice formation. The four types are:

- free water saturating the pores larger than 100 nm; its structure is not influenced by the fluid-solid interface, and thus the freezing point is at 0°;

- capillary-condensed water saturating the 10–100 nm pores; this is influenced by the capillary forces and freezes at about −15°;

- structured water saturating the 3–10 nm pores; it freezes at about −43°;

- adsorbed water saturating the pores smaller than 3 nm; it forms about 2.5 monomolecular layers on the solid surface, and freezes at −160°.

Low-temperature thermal expansion of water-saturated porous materials

Low-temperature thermal expansion measurements are used in silicate research for both theoretical and practical reasons. One special field of application of low-temperature dilatation measurements is the research into porous materials exposed to weather conditions. In this case, the low-temperature thermal expansion of a water-saturated porous sample is measured. The dilatation curve depends on the characteristics of the solid matrix material, the pore structure, the saturating rate and the characteristics of the water.

Two main types of construction materials have been investigated via low-temperature dilatation measurements. Lehmann *et al.* reviewed the entire field of the low-temperature thermal expansion behaviour of ceramics and sand-lime brick [4, 10]. Results on the relationship between pore volume, strength and frost dilatation effects for ceramic matrix materials were published earlier [7].

Research on cement-containing materials was reported in Litvan's publications, where the aim was a reduction of the time needed for standard frost resistance tests [12–14]. A theory of frost action in cement paste has been proposed in connection with dilatation measurements [15].

Both Lehmann and Litvan tried to find a relationship between frost resistance and residual expansion after several cooling and heating cycles. How-

ever, although there were some encouraging results, the traditional frost resistance tests involving freeze-thaw cycles could not be replaced by low-temperature dilatation tests.

In the present work, the characteristics of the entire low-temperature dilatation curves will be discussed in relation to the pore size distribution.

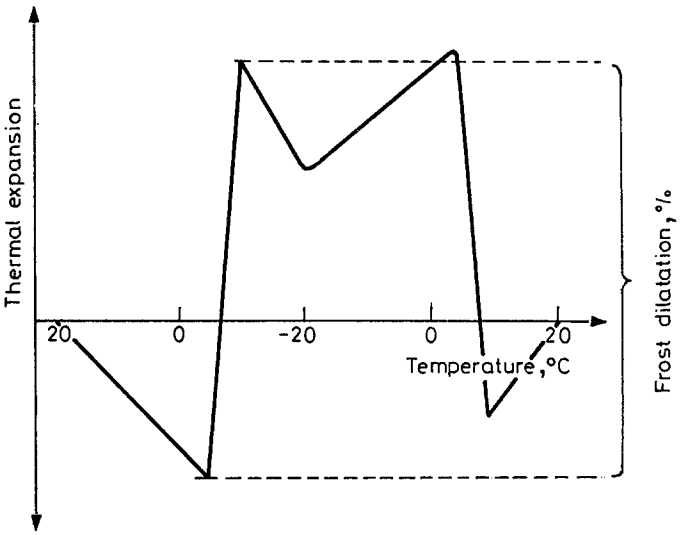

Fig. 1 Schematic low-temperature dilatation curve of a water-saturated porous material

Special attention will be paid to the "frost dilatation effect" (which is the expansion due to the freezing of water, shown in Fig. 1).

Experimental

The experiments were carried out on traditional Portland cement and on a special, gypsum-free, high-strength (MNC) cement. The ordinary Portland cement used for comparisons was ground from plant clinker in a laboratory mill to a surface area of 300 m^2/kg by Blaine. The chemical and mineral compositions of the cement clinker can be found in Table 1a-b.

The same clinker (but with different additives) was used for the special cement, but the surface area was much higher (566 m^2/kg). Some characteristic data concerning the grain size distribution are listed in Table 2.

4% gypsum was added to the traditional Portland cement in order to regulate the setting time. In the case of the MNC cement, a mixture of lignosulphonate and alkali metal carbonate was added instead of gypsum. This

Table 1a Chemical composition of the cement clinker (Abbrevations applied in cement chemistry: C_3S: tricalcium-silicate, C_2S: dicalcium-silicate, C_4AF: tertacalcium-aluminate-ferrite C_3A: tricalcium-aluminate; silicate modulus: SiO_2/Al_2O_3, aluminate modulus: Al_2O_3/Fe_2O_3

Chemical composition	
Ignition loss at 1000°C	1.1 %
SiO_2 + insoluble residue	22.0 %
Al_2O_3	6.1 %
Fe_2O_3	3.5 %
TiO_2	0.3 %
CaO	64.3 %
MgO	1.2 %
K_2O	0.7 %
Na_2O	0.2 %
SO_3	0.1 %
Free CaO	0.4 %
Silicate modulus	2.29 %
Aluminate modulus	1.74 %
Saturation factor	0.85 %

Table 1b Mineral composition of the cement clinker

Mineral composition	Calculated by Bogue's method	Measurement by X-ray diffraction method
	%	%
C_3S	46.2	44
C_2S	28.2	16
C_4AF	10.6	8
C_3A	10.2	2

mixture allowed regulation of the setting time and the strength, and at the same time a reduction of the amount of water required to ensure workability [16].

Prism specimens were cast from both cement pastes. The water-to-cement ratios were 0.31 and 0.26 for the traditional Portland cement and MNC cement, respectively. After demoulding at the age of 1 day, 5×5×50 mm

Table 2 Grain size distribution data of the Portland and MNC cement applying the Rosin-Ramler approach

	Portland cement	"MNC" cement
"X" characteristic grain size, μm	21	8
"n" uniformity ratio	0.899	0.913
for fraction of 1 μm, %	7.3	15.8
for fraction of 3 μm, %	15.1	28.7
for fraction of 3–30 μm, %	61.2	70.2
Specific surface area by Blaine's method in m^2kg^{-1}	300	566

prism-shaped samples were cut for dilatation measurements. This small sample size is advantageous as concerns the temperature gradient in the sample during cooling, but disadvantageous from the point of view of a representative sample. The samples were cured at room temperature in a

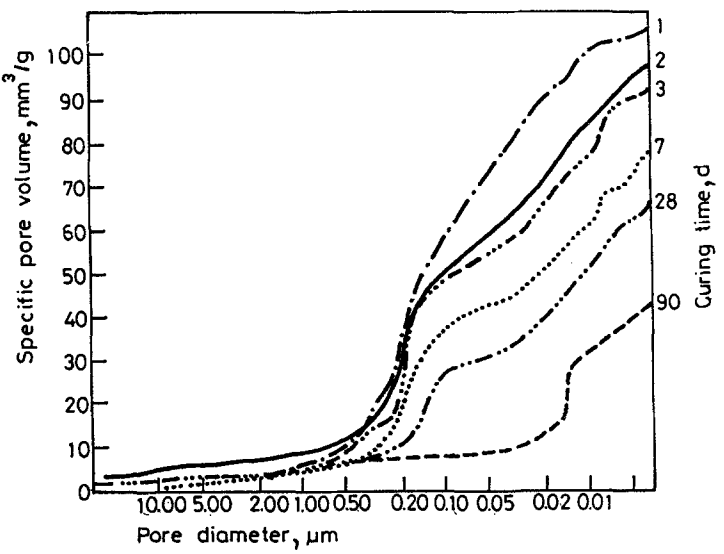

Fig. 2 Cumulative porosity curves of hydrated Portland cement pastes

Table 3 Porosity data of hydrated cement pastes

Sample	Curing time, day	Specific pore volume in the 0.005–1.77 μm pore diameter range, cm^3g^{-1}	Specific pore volume in the micropores in the 0.005–0.0036 μm pore diameter range, cm^3g^{-1}	Median pore diameters of the characteristic pore ranges, μm			Specific pore volume of the characteristic pore ranges, cm^3g^{-1}		
				surface pores	macro-pores	meso-pores	surface pores	macro-pores	meso-pores
Portland cement									
	1	0.1040	0.0031		0.12			0.1040	
	2	0.0940	0.0041	8.0	0.170	0.015	0.010	0.049	0.033
	3	0.0900	0.0021		0.170	0.012		0.054	0.031
	7	0.0720	0.0068		0.170	0.013		0.038	0.028
	28	0.0616	0.0056		0.130	0.013		0.024	0.031
	90	0.0390	0.0052			0.013			0.030
MNC cement									
	1	0.0668	0.0052	0.4	0.065	0.012	0.011	0.0255	0.025
	2	0.0595	0.0068	0.4	0.080	0.012	0.008	0.0195	0.022
	3	0.0535	0.0053	0.38	0.075	0.010	0.011	0.0140	0.024
	7	0.0381	0.0074		0.025	0.011		0.0070	0.015
	28	0.0294	0.0074		0.050	0.006		0.0090	0.012
	90	0.0205	0.0085		0.009			0.012	

water-saturated atmosphere until the measurements. The experiments were carried out on pastes aged 1, 2, 3, 7, 28 and 90 days.

Porosity measurements were carried out with a MICROMERITIC 915 mercury penetration porosimeter. The pressure range of the porosimeter is between 7 kPa and 345 MPa. Thus, a pore diameter range of from 4 nm to 0.177 mm can be covered by applying a 130° mercury contact angle for the material examined, and 0.474 N/m as the surface tension in Washburn's equation.

In mercury porosimetry, the compressibility of mercury results in errors in the pressure range 20 to 345 MPa (i.e. 4–60 nm pore diameter). A correction must be applied for this or the porosity measurement will be false in the range of meso- and micropores. An empirical correction method was developed earlier to ensure reliable porosity results [17]. Prior to the porosity measurements, samples were dried in vacuum at room temperature.

Low-temperature dilatation curves were measured on a Netzsch ET 402 vertically arranged quartz dilatometer, in the temperature range +20 to −100° with cooling and heating rates of 2 deg/min. Prior to the experiments, the samples were vacuum-saturated and covered with a flexible film to avoid water loss during the measurement.

Results and discussion

Pore structure of hydrated cement pastes

The cumulative porosity curves of the hydrated cement pastes at different stages of hydration are presented in Figs 2 and 3.

The pore size distributions of the hydrated cement pastes are in agreement with the findings of the Parcevaux [2]. With only one exception, all the pore types can be seen in the curves. The exception is the porosity curve for the traditional cement paste at the age of 1 day, when the characteristic pore types had not yet developed, so the pore size ranges of macro- and mesopores could not be distinguished (see Fig. 2).

The pore size distribution of the hydrated MNC cement was similar to that of the traditional Portland cement pastes, but the range of macropores could be divided into two groups at the age of 1–3 days.

The median pore size and specific pore volume of the characteristic pore size ranges are listed in Table 3 to demonstrate the pore size and pore volume changes during hydration. The range of micropores is shown separately, because the range of mercury porosimetry covers only part of the

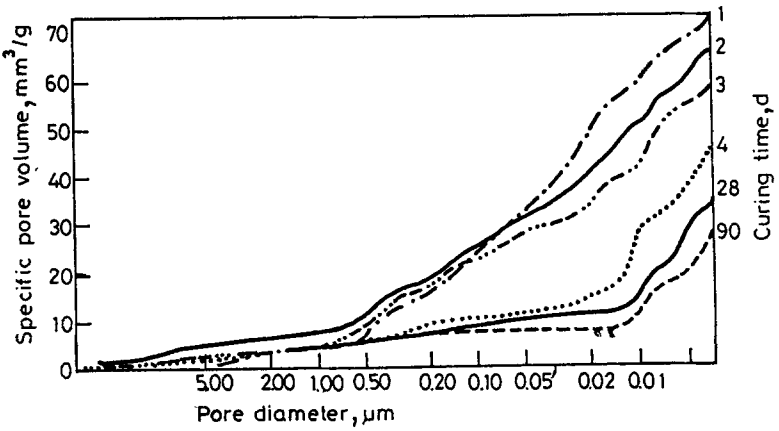

Fig. 3 Cu.mulative porosity curves of hydrated MNC cement pastes

range of micropores, and thus the specific pore volume measured does not involve the volume of all micropores.

The specific pore volume decreased with increasing curing time in the course of the hydration process, mainly because of the decrease in the number of macropores, but there were slight decreases in the number and median pore size of the mesopores as well.

An extremely low specific pore volume was found in the early stage of hydration of the MNC cement.

Low-temperature dilatiation of water-saturated hydrated cement pastes

The low-temperature dilatation curves of the samples at different stages of hydration are shown in Figs 4 and 5. Two separate expansion effects can be seen in the cooling curves of those specimens in which both macro- and mesopores have considerable volumes, when the pore size distribution and the low-temperature dilatation behaviour of the samples are compared.

An extremely high expansion effect occurred without separate freezing in the macro- and mesopores when the characteristic pore structure had not yet developed (traditional paste at the age of 1 day), but overall expansion remained until the age of 7 days. MNC pastes, on the other hand, showed no expansion, even at early ages.

The temperatures of the expansion effects measured are in agreement with the DTA results of Dorner and Setzer [3], but the values are lower then the real freezing points, because the temperature is measured in the surroundings and not inside the sample.

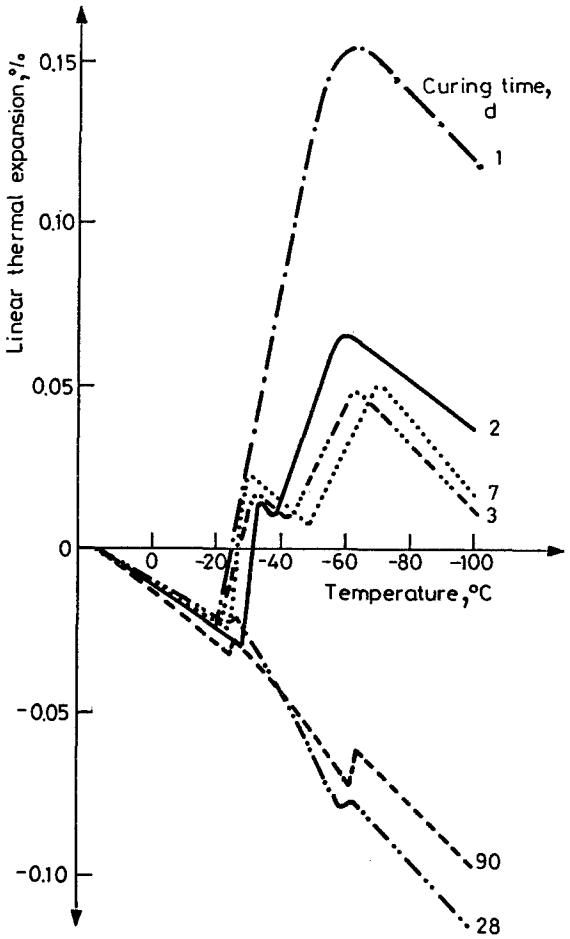

Fig. 4 Low-temperature dilatation curves of hydrated Portland cement pastes

The measure of the expansion effect (cf. the distance between the minimum and the maximum of the dilatation curve) is called the "frost dilatation" (see Fig. 1). The frost dilatation results are given in Table 4.

A comparison of the specific pore volume and frost dilatation values permits the conclusion that there is not a linear relationship between the two sets of data. The measure of the expansion is influenced by the pore volume, i.e. by the volume of saturating water, and by the strength of the matrix material enclosing the pores. It must be emphasized that the measure of the expansion is one magnitude less than the theoretical value, derived from the 9.02% volume expansion of freezing water saturating the pore types in ques-

Table 4 Frost dilatation values of hydrated cement pastes

Sample	Curing time	Frost dilatation effect	
		at $-15^{\circ}C$	at $-40^{\circ}C$
	day	%	%
Portland cement	1	0.1786	
	2	0.0456	0.0553
	3	0.0407	0.0386
	7	0.0473	0.0416
	28	0.0037	0.0
	90	0.0035	0.0110
MNC cement	1	0.0111	0.0296
	2	0.0082	0.0401
	3	0.0085	0.0299
	7	0.0024	0.0287
	28	0.0011	0.0045
	90	0.0025	0.002

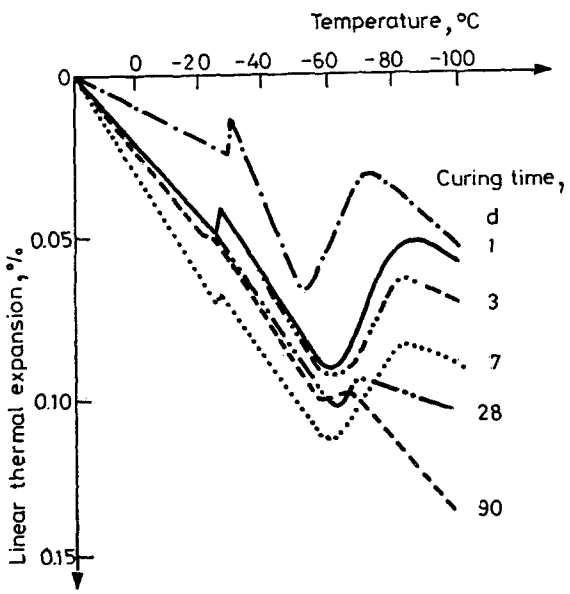

Fig. 5 Low-temperature dilatation curves of hydrated MNC cement pastes

tion. It was shown in an earlier publication that the frost dilatation for ceramic matrix material is influenced not only by the volume of saturating water, but also by the strength of the solid matrix [7].

The effect of the strength of the solid matrix can be observed for both samples: in the course of hydration, a considerable decrease in the second frost dilatation effect could be observed, although the volume of the mesopores did not decrease similarly.

* * *

The author is grateful to Dr. Ludmilla Opoczky and Mr. Imre Horváth for the samples.

References

1 M. M. Dubinin *et al.*: Zhur. Fiz. Khim., 34 (1960) 2019.
2 P. Parcevaux, Cement Concr. Res., 14 (1984) 419.
3 H. W. Dorner and M. Setzer, Cement Concr. Res., 10 (1980) 403.
4 H. Lehmann, Ziegelind., 8 (1955) 569.
5 H. Lehmann and H. Feldmann, Ziegelind., 10 (1957) 365.
6 H. Lehmann and W. Ohnemüller, Ziegelind., 12 (1959) 735.
7 H. Lehmann, S. Traustel and W. Ohnemüller, Tonind. Z., 84 (1960) 219.
8 H. Lehmann and W. Ohnemüller, Tonind. Z., 84 (1960) 457.
9 H. Lehmann and E. Rauschenfels, Ziegelind., 23 (1970) 337.
10 H. Lehmann and E. Rauschenfels, Tonind. Z., 94 (1970) 177.
11 Zs. E. Wagner, Interbrick, 5 (1989) 23.
12 G. G. Litvan, J. Colloid. Interface Sci., 38 (1972) 75.
13 G. G. Litvan, J. Amer. Ceram. Soc., 5 (1973) 38.
14 G. G. Litvan, J. Colloid. Interface Sci., 45 (1973) 154.
15 G. G. Litvan, Mater. Constr., 6 (1973) 293.
16 L. Opoczky, L. Horváth and L. Szatura, Proc. XVth Conf. on Silicate Industry and Silicate Science (SLIFCONF) Budapest, 12-16 may 1989.
17 Zs. E. Wagner, Powder Technology, 35 (1973) 83.

Zusammenfassung— An einem herkömmlich hydratierten Portland Zementleim und einem Spezialzementleim mit hoher Anfangsfestigkeit wurde die Porenstruktur und das Dilatationsverhalten bei niedrigen Temperaturen untersucht. Mit dieser Untersuchung sollte gezeigt werden, welche Rolle die Zementart während des Hydratationsprozesses bei der Ausbildung der Porenstruktur und der Ausdehnung bei Frost spielt. Die geringere Porösität und höhere Festigkeit des speziell hydratierten Zementleimes ergaben bezogen auf herkömmlichen Zementleim im frühen Stadium der Hydratation geringere Dilatationseffekte bei Frost.